Muscone Attenuates Uveitis Through the PI3K/AKT Signaling Pathway

Xianyang Liu,[1,2] Hangjia Zuo,[2] Chao Wu,[1] Na Li,[3] Qian Zhou,[2] Fan Cao,[1] Baorui Chu,[1] Shuhao Zeng,[1,2] Hui Feng,[1] Yakun Wang,[1,2] Fengyang Lei,[1] Ke Hu,[2] and Shengping Hou[1]

[1]Beijing Institute of Ophthalmology, Beijing Tongren Eye Center, Beijing Tongren Hospital, Capital Medical University, Beijing Ophthalmology & Visual Sciences Key Laboratory, Beijing, China
[2]The First Affiliated Hospital of Chongqing Medical University, Chongqing, China
[3]Department of Laboratory Medicine, Beijing Tongren Hospital, Capital Medical University, Beijing, China

Correspondence: Shengping Hou, Beijing Institute of Ophthalmology, Beijing Tongren Hospital, Capital Medical University, No. 17, Hougou Alley, Dongcheng District, Beijing 100730, China; sphou828@163.com.

XL, HZ, and CW contributed equally to this work.

Received: November 25, 2024
Accepted: April 15, 2025
Published: May 9, 2025

Citation: Liu X, Zuo H, Wu C, et al. Muscone attenuates uveitis through the PI3K/AKT signaling pathway. *Invest Ophthalmol Vis Sci.* 2025;66(5):21. https://doi.org/10.1167/iovs.66.5.21

Purpose. Uveitis is an immune-mediated ocular disorder that poses a significant threat to vision, particularly among young and middle-aged adults. The treatment of uveitis is complicated by the presence of the blood-retinal barrier (BRB), which restricts the passage of large molecular drugs into the eye, thus limiting effective therapeutic options. The primary objective of this study is to identify a novel therapeutic agent capable of treating uveitis and explore its underlying mechanism.

Methods. In this study, we used a mouse model of experimental autoimmune uveitis (EAU) induced by interphotoreceptor retinoid-binding protein (IRBP) and lipopolysaccharide (LPS) and interferon-gamma (IFN-γ)-induced inflammatory BV2 cells. Evans blue and fundus fluorescein angiography (FFA) experiments were performed to evaluate the destruction of BRB. Silt lamp and hematoxylin and eosin (H&E) staining were conducted to evaluate the inflammatory response. In vivo proteomics and Western blot were carried to investigate the underlying mechanisms.

Results. Our study reveals that Muscone significantly alleviates EAU and restores the integrity of BRB. Moreover, Muscone treatment markedly downregulated inflammatory factors within the retinas and BV2 cells. In vivo proteomic combined with liquid chromatography-mass spectrometry (LC-MS) has elucidated that Muscone exerts its anti-inflammatory effects by modulating the PI3K-AKT signaling pathway. Moreover, by using LY294002 to specifically inhibit PI3K, we observed a marked decrease in inflammatory phenotype and BRB destruction of EAU.

Conclusions. In summary, this study establishes the protective efficacy of Muscone against the progression of EAU and provides insights into the molecular mechanisms responsible for its therapeutic action.

Keywords: uveitis, microglia, muscone, proteomics, PI3K/AKT pathway

Uveitis is a common eye disease with a high potential for blindness, which can occur at any age but is particularly prevalent among young and middle-aged individuals between the ages of 20 and 50 years.[1] Reports indicate that, in developed countries, 5% to 15% of legally blind cases can be attributed to uveitis.[1,2] Uveitis, categorized into four types based on its anatomic location, anterior uveitis typically presents with pain, redness, blurred vision, photophobia, tearing, floaters, changes in pupil shape, swollen conjunctiva, and hypopyon; intermediate uveitis is characterized by floaters, blurred vision, mild redness, and visual field defects; posterior uveitis manifests with blurred vision, photophobia, visual field loss, retinal vasculitis, optic disc swelling, and macular edema; and panuveitis involves the entire uvea.[3,4] The etiology of the disease is complex and diverse, resulting from infections by various pathogens such as bacteria, viruses, fungi, and parasites, as well as factors like autoimmune and genetic conditions.[3,5]

The treatment of uveitis remains challenging at present, primarily due to the complex etiology and pathogenesis of this disease.[6] A variety of medications are commonly used to manage uveitis, including glucocorticoids, immunosuppressants, biologics, and nonsteroidal anti-inflammatory drugs.[6–8] Among these, biologics that target specific cytokines, such as IL-6 inhibitors (e.g. tocilizumab) and IL-17 inhibitors (e.g. secukinumab), have emerged as a promising approach, particularly for treating non-infectious uveitis that is resistant to conventional therapy.[9] It is worth noting that a significant number of patients achieve sustained remission following appropriate immunosuppressive therapy, with the rates of remission varying depending on the specific subtype and etiology of uveitis.[10,11]

With the advancement of modern science and technology, traditional Chinese medicine has entered a new stage of development.[12–14] Modern analysis has shown that the integration of traditional Chinese and Western medicine can

reduce the side effects of drugs during the treatment process and achieve better therapeutic effects.[15] The combination of traditional Chinese and Western medicine has therapeutic effects on uveitis and is considered to be relatively safe.

Muscone is a medicinal material obtained from the musk glands of musk animals and has excellent pharmacological activity.[16] Studies have reported that musk has therapeutic effects on various diseases, including the central nervous system and the cardiovascular system.[16–18] Additionally, it can rapidly pass through the blood-brain barrier or the blood-retinal barrier (BRB) to exert anti-inflammatory effects directly at the pathological core.[19] Muscone is the main active component of musk, exhibiting strong anti-inflammatory properties.[20] These groundbreaking studies provide new strategies and hope for the clinical treatment of uveitis.

In this study, we found that Muscone alleviates experimental autoimmune uveitis (EAU)-related inflammation and helps restore the integrity of the blood-retinal barrier (BRB). It also suppresses the M1 phenotypic polarization of microglia in the retina and BV2 cells. Mechanically, in vivo proteomic and liquid chromatography-mass spectrometry (LC-MS) analysis showed that Muscone regulates EAU inflammation through the PI3K-AKT signaling pathway. Taken together, this study identified the protective effects of Muscone on EAU progression and provided a novel therapeutic agent.

Materials and Methods

Animals

Female C57BL/6J mice, aged between 6 and 8 weeks and weighing approximately 16 to 18 grams, were sourced from the Experimental Animal Center at Chongqing Medical University. All animal-related procedures were conducted in strict accordance with the guidelines set forth by the Ethics Committee of the First Affiliated Hospital of Chongqing Medical University (Approval number: 2019-296). Additionally, the research adhered to the Association for Research in Vision and Ophthalmology's Statement for the Use of Animals in Ophthalmic and Vision Research.

Cell Culture and Reagents

The microglial cell line (BV2) was obtained from the American Type Culture Collection (ATCC). These cells were cultured in a humidified incubator maintained at a constant temperature of 37°C, with a consistent 5% CO_2 supply. The growth medium used was Dulbecco's Modified Eagle Medium (DMEM; Gibco), enriched with 10% fetal bovine serum (FBS) and 0.5% penicillin-streptomycin (P/S; Procell Life Science & Technology Co., Ltd.). Serum-free cell freezing medium was purchased from Witcel (A401, Shanghai). The cell cryopreservation tube was purchase from A-GEN. Lipopolysaccharides (LPS) and interferon-γ (IFN-γ) were sourced from PeproTech (Thermo Fisher Scientific, Inc., USA). Dimethyl Sulfoxide (DMSO) was purchased from Sigma-Aldrich. Muscone was obtained from Selleck Chemicals (S3871, USA). Fluorescein sodium salt was acquired from Aladdin (Shanghai, China). LY294002 was purchased form MCE.

The BV2 cells that remained untreated served as the control group. The BV2 cells were treated with a combination of LPS (1 µg/mL) and IFN-γ (100 ng/mL) for a duration of 24 hours, representing the stimulated group. In the experimental group, the BV2 cells were pre-treated with Muscone at concentrations of 10 µM and 20 µM for 2 hours prior to the stimulation with LPS (1 µg/mL) and IFN-γ (100 ng/mL) for an additional 24 hours.

Induction of Experimental Autoimmune Uveitis

In our study, the mice were subjected to immunization with a precise dosage of 500 µg of human interphotoreceptor retinoid-binding protein ($IRBP^{651-670}$) peptide (sequence: LAQGAYRTAVDLESLASQLT).[5,21–23] Concurrently, 1 µg of Bordetella pertussis toxin was administered intraperitoneally, following the established protocols. The mice that developed EAU were then randomly assigned into two distinct groups. The first group of EAU mice was given Muscone intraperitoneally at a dosage of 20 mg/kg body weight, starting from day 7 to day 13 post-immunization, with administrations occurring every other day. The second group received an intraperitoneal administration of the vehicle saline solution supplemented with 1% DMSO in an equivalent volume (200 µL per mouse). Non-immunized mice served as the control group.

Intravitreal Injection

The sterile injection procedure adhered to previously established protocols. To summarize, the mice were subjected to intraperitoneal injections of 1% pentobarbital sodium (50 mg/kg) and 0.5% tropicamide to induce anesthesia. A precise incision was meticulously created at a distance of approximately 1.0 to 2.0 mm from the corneoscleral limbus, utilizing a 29-gauge needle. A blunt-tipped 29-gauge needle (Hamilton, CA, USA) was then delicately inserted into the vitreous cavity through the incision, and LY294002 (10 µM/mL) was administered gradually. The needle was subsequently withdrawn with a gentle motion, following a brief pause. Postoperatively, antibiotic ointment was applied to the cornea daily for a continuous period of 3 days to prevent infection.

Clinical Scores and Pathological Scores

The anterior segment scores were evaluated based on five independent criteria, as previously described, in a blinded manner to ensure the objectivity of the results.[24] Fundus clinical scores were similarly assessed according to Caspi's criteria, also in a blinded manner to maintain the integrity of the study.[25] At the apex of the inflammatory response, which occurred on day 14 of the study, all mice were humanely euthanized to facilitate further analysis.

Hematoxylin and Eosin Staining

Tissues were stained with Harris' hematoxylin for 6 hours at 60°C to 70°C, followed by thorough rinsing in tap water to remove excess stain. The tissues were then treated with a solution of 10% acetic acid and 85% ethanol for 2 cycles: 2 hours and 10 hours, respectively. After each cycle, the tissues were rinsed with tap water. The bluing step was performed in a saturated lithium carbonate solution for 12 hours, followed by a final rinse in tap water. Staining was completed with an eosin Y ethanol solution for 48 hours. Microscopic images were captured using a Leica microscope (Leica, Germany).

Investigative Ophthalmology & Visual Science

Retinal Immunofluorescence

The eyes of the mice were immersed in a 4% paraformaldehyde (abs9179, Absin) solution and allowed to fix at room temperature for a duration of 2 hours. Once fixed, the surrounding extraneous tissues were meticulously excised, and the retina was delicately dissected into a precise quadrifoliate configuration. The cell membranes were permeabilized to facilitate access to intracellular antigens, followed by a blocking step with goat serum (Bio Channel Bio Technology) for 30 minutes at a temperature of 37°C. After gently removing the blocking solution, the tissue sections were incubated with the IBA1 antibody, which serves as a specific marker for microglia (at a dilution of 1:350). The slides were subsequently placed flat within a humidified chamber, ensuring an optimal environment for antibody binding, and incubated at 4°C overnight. Subsequently, the sections were incubated with the Cy3 fluorescent-conjugated secondary antibody (Beyotime, Shanghai, China) for 1 hour at room temperature to form a visible complex. Images were captured with a high-resolution fluorescence microscope (Leica, Germany).

Assessment of the Blood-Retinal Barrier

The breakdown of the BRB was evaluated by Evans blue analysis and fluorescein fundus angiography (FFA) on day 14 after immunization. The mice were gently sedated, followed by an intraperitoneal injection of 10% fluorescein sodium salt solution, and the resulting images were captured.

For the Evans blue analysis, the mice were injected with a 2% Evans blue solution (Sigma-Aldrich, USA) via the tail vein. After a period of 2 hours, the animals were humanely euthanized. Their eyes were then fixed in a 4% paraformaldehyde solution for 2 hours. Then, the retinas were carefully dissected, mounted with glycerol onto glass slides, and covered with coverslips to prepare for microscopic examination. The images of the stained retinas were collected using a confocal laser scanning microscope (Olympus, Japan).

Protein Preparation, Digestion, and Peptide Labeling

Protein extraction followed a published protocol. Tissue was homogenized in a lysis buffer (8 M urea, 2 M thiourea, 4% CHAPS, 20 mM Tris - base, 30 mM DTT, and Roche protease inhibitors) at 1 mg/10 µL on ice. After centrifugation at 15,000 g and 4°C for 20 minutes, the supernatant was precipitated with 3-fold cold acetone for 30 minutes, and then centrifuged again under the same conditions. Pellets were resuspended in 100 µL of 5 M urea and dissolved in four volumes of 40 mM NH4HCO3. Protein concentration was measured using a BCA assay. The sample was treated with 10 mM DTT for 1 hour to cleave disulfide bonds, followed by alkylation in the dark with 50 mM iodoacetamide for 1 hour at room temperature. Proteins were digested with sequencing-grade trypsin (enzyme-to-protein ratio of 1:50) at 37°C for 14 hours, then the reaction was stopped with formic acid. Peptides were concentrated using a SpeedVac system and labeled with TMT reagent for 1 hour at room temperature, followed by quenching with hydroxylamine for 15 minutes according to the kit's manual. Labeled samples were pooled and stored at –80°C.

LC-MS Analysis

Peptide samples were analyzed using a high-resolution LC-MS system, specifically the U3000 nano HPLC system and Q-Exactive mass spectrometer (both from Thermo Fisher Scientific, USA), configured with a nano electrospray source. For peptide enrichment, reverse-phase chromatography was performed on a 2-cm-long, 75 µm i.d. fused silica trap column packed with 3.0 µm Aqua C18 resin beads (Thermo Fisher Scientific). Peptides were loaded at 5 µL/min and then eluted from a 25-cm-long, 75 µm i.d. analytical column packed with 2.0 µm Aqua C18 beads using a gradient elution at 300 nL/min. The gradient started at 100% buffer A (0.1% formic acid), increased to 3% buffer B (0.1% formic acid and 99.9% acetonitrile) over 5 minutes, then to 18% buffer B over 31.5 minutes, followed by a step to 30% buffer B over 2 minutes, and finally to 80% buffer B for 5 minutes. Eluted peptides were introduced into the mass spectrometer's nano-ESI source. Full scan resolution was set at 70,000 (m/z range 350–1600), and tandem mass spectrometry (MS/MS) scans were performed at a resolution of 3500 with an isolation window of 2 m/z, normalized collision energy of 29, and a loop count of 20. Dynamic exclusion parameters were applied to enhance efficiency and prevent redundant sequencing. The MS/MS data were stored in RAW format using Xcalibur software (version 2.2, Thermo Fisher Scientific).

Quantitation of Protein Abundance

Raw MS data were processed using Proteome Discoverer 2.3 (Thermo Fisher Scientific) to quantify protein abundance. Feature detection was performed via the expectation-maximization algorithm, and alignment of identical peptides across samples was achieved using a high-performance retention time algorithm. Retinal protein levels were quantified and compared based on the sum of the three most intense tryptic peptide ions. Statistical significance was determined by a P value < 0.05 and a fold change ≥ 1.5. Differentially expressed proteins between the EAU and EAU + Muscone groups were profiled via hierarchical clustering and visualized using heatmap.2.

Bioinformatics Analysis

To further characterize the biological groups and pathways associated with the identified proteins, we utilized the OmicsBean software via its online platform at http://www.omicsbean.cn/. Gene Ontology (GO) category enrichment was assessed using a right-sided hypergeometric test, comparing the identified proteins to the GO annotations across the Mus musculus genome. The false discovery rate (FDR) was controlled using the Bonferroni step-down method to ensure confidence in the enriched GO categories. Proteins were grouped according to their GO annotations, with significant categories defined by P values less than 0.05.

Cell Viability Assay

The BV2 cells viability was evaluated using the CCK8 assay, following the protocol provided by the manufacturer. Cell quantification was performed using a cell counter (Countstar, China). Cells were plated at a concentration of

Investigative Ophthalmology & Visual Science

5×10^3 per well in 96-well plates, each filled with 100 µL of DMEM medium. After undergoing the designated treatments, the CCK8 reagents (C0005, TargetMol, USA) were introduced into the culture medium and allowed to incubate for 2 to 3 hours. Thereafter, the optical density for each well was quantified at a wavelength of 450 nm, using a microplate reader (Thermo Fisher Scientific, Inc., Waltham, MA, USA).

EdU Proliferation Assay

The cell proliferation was assessed through the EdU Staining Proliferation Kit from Beyotime, Shanghai, China. Initially, 5×10^4 cells were seeded into each well of a 24-well plate (BDBIO HangZhou China). Once the cells had adhered to the surface, they were subjected to the respective treatments. Subsequently, the cells were treated with a 50 µM EdU reagent for 2 hours and then fixed with a 4% paraformaldehyde solution for 30 minutes. After fixation, the cells were permeabilized by incubation in 0.5% Triton X-100 (Biosharp) for 20 minutes. The cells were then incubated with a 200 µL reaction mixture provided by the EdU kit for 30 minutes, followed by staining with 1X Hoechst 33342 (23491-52-3, Cytoch) for 5 minutes. The proportion of EdU-positive cells was captured using fluorescence microscopy (Leica, Germany).

Transwell Assay

The BV2 cells were cultured in the upper chamber of Corning Transwell systems (Corning Inc., Corning, NY, USA), at a seeding density of 2×10^4 cells per well. Once the cells had firmly attached to the surface, the upper compartment was treated with either none, LPS + IFN-γ, or a combination of LPS, IFN-γ, and Muscone. After a 24-hour incubation period, the BV2 cells in the upper compartment were gently washed twice with PBS to remove any non-adherent cells. They were then fixed with a 4% paraformaldehyde solution for 10 minutes and stained with 0.1% crystal violet (Beyotime, Shanghai) for 20 minutes. The cells on the upper surface were carefully removed, leaving the cells on the lower surface intact for imaging. The lower surface cells were photographed, and the staining was quantified using ImageJ software.

Western Blotting

BV2 cells were cultured in 6-well plates (Jet Biofil, Guangzhou) and subjected to various treatments. After the treatments, the cells were gently washed twice with PBS to remove any residual substances. Pre-cooled lysis buffer (R0010, Solarbio) was then added to lyse the retina or BV2 cells. The protein concentration within these samples was quantified using the Bicinchoninic Acid Kit (Beyotime, Shanghai, China). The proteins were resolved by gel electrophoresis and subsequently transferred onto a polyvinylidene fluoride (PVDF) membrane. The membrane was blocked with Fast Blocking Western reagent (Yeasen, Shanghai) to prevent non-specific binding. After blocking, the membrane was gently washed with Tris-buffered saline-Tween 20 (TBST) to prepare it for incubation with primary antibodies. The membrane was then incubated at 4°C overnight to allow for optimal antibody binding to the target proteins. Finally, the protein bands were visualized using an ECL kit (KF8001, Affinity). The intensity of the bands was quantified using Image J software. The primary antibodies used in this study are listed in Supplementary Table S1.

Statistics Analysis

All experiments were replicated at least three times for reliability and reproducibility. We used the Unpaired Student's *t*-test for two group comparisons and 1-way ANOVA for multiple groups. The Mann-Whitney *U* test was applied to clinical and pathological scores. Statistical significance was set at $P < 0.05$. Data are presented as mean ± SD, analyzed using SPSS 27 (IBM Corp., Armonk, NY, USA) and Prism 9.0 (GraphPad, USA).

Results

Muscone Alleviates Retinal Inflammation in EAU Mice

To explore Muscone's effect on autoimmune uveitis, EAU mice were treated with intraperitoneal Muscone (20 mg/kg) starting on day 7 post-induction and every other day until day 14, after which the retinas were collected (Fig. 1A). The structure of Muscone is depicted (Supplementary Fig. S1). Body weight was monitored from day 7, with no difference observed among the Muscone, the control, and the DMSO groups (Fig. 1B). Clinical images revealed severe conjunctival and ciliary hyperemia in the EAU + DMSO group compared with the controls, whereas the EAU + Muscone group showed milder symptoms (Figs. 1C, 1E). Hematoxylin and eosin (H&E) staining indicated more retinal folds and inflammatory cells in the EAU + DMSO group, with fewer observed in the EAU + Muscone group after treatment (Figs. 1D, 1F). Western blotting showed increased levels of inflammatory cytokines (iNOS, IL-6, and IL-1β) in the retinas post-immunization (Fig. 1G), which were significantly reduced by Muscone treatment (Fig. 1H).

Microglia, the resident immune cells in the retina and central nervous system, are crucial for maintaining retinal homeostasis and immune surveillance.[26] Immunofluorescence staining of retinal flat mounts revealed a reduced number of microglia with Muscone treatment (Figs. 1I, 1J). Consistently, the EAU group exhibited elevated protein expression levels of IBA1 and CD68 (Fig. 1K). Notably, treatment with muscone led to a significant reduction in these elevated levels (Fig. 1L).

Muscone Protects the Function of the Blood-Retinal Barrier

The BRB is a crucial protective structure in the eye. It protects the retina from harmful substances in the bloodstream while maintaining selective permeability, facilitating the efficient removal of metabolic waste via active transport.[27] In diseases like uveitis, the BRB's integrity is compromised, making the retina more vulnerable to damage, including inflammation-induced cellular injury.[28,29]

The FFA and Evans blue assay showed aggravated retinal vessel leakage in EAU mice. However, Muscone treatment alleviated this leakage (Figs. 2A, 2B). Additionally, we measured the expression of Occludin, a key protein for tight junction function. Occludin levels were significantly higher in EAU mice than in the healthy controls (Fig. 2C), but Muscone treatment notably decreased Occludin protein levels in EAU mice (Fig. 2D).

Investigative Ophthalmology & Visual Science

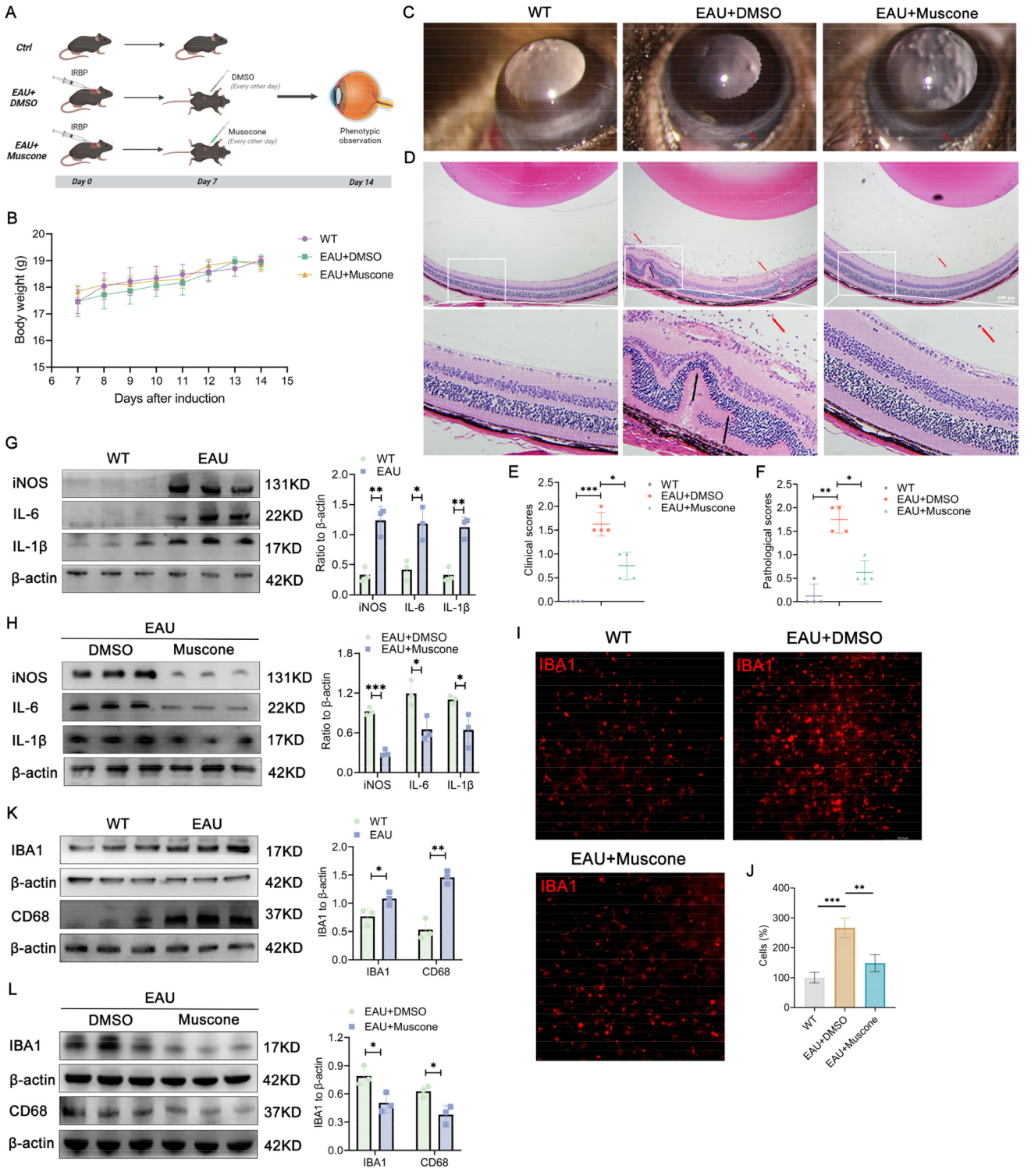

Figure 1. Muscone effectively mitigates retinal inflammation in mice with EAU. (**A**) Schematic depiction of the post-immunization treatment procedure with DMSO or Muscone in mice. (**B**) Comparative body weight tracking across different treatment groups including control mice, EAU mice with DMSO, and EAU mice with Muscone. (**C, E**) Clinical scores of control mice, EAU mice with DMSO, and those treated with Muscone (mean ± SD; $n = 4$/group; $^{*}P < 0.05$, $^{***}P < 0.001$; Mann-Whitney U test; *red arrow* = ciliary congestion). (**D, F**) Pathological scores in the same groups mentioned above (mean ± SD; $n = 4$/group; $^{*}P < 0.05$, $^{**}P < 0.01$; Mann-Whitney U test; *red arrow* = inflammatory cells, *black arrow* = retinal folds). (**G**) Protein levels and quantitative chart of iNOS, IL-6, and IL-1β in retinal tissues between control and EAU mice (mean ± SD; $n = 3$/group; $^{*}P < 0.05$, $^{**}P < 0.01$, unpaired Student's t-test). (**H**) Protein levels and quantification of iNOS, IL-6, and IL-1β in retinal tissues between EAU mice and EAU mice with Muscone (mean ± SD; $n = 3$/group; $^{*}P < 0.05$, $^{***}P < 0.001$, unpaired Student's t-test). (**I, J**) Immunofluorescence visualization of the microglial marker IBA1 in retinas from control, EAU, and EAU with Muscone groups (mean ± SD; $n = 3$/group; $^{***}P < 0.001$, $^{**}P < 0.01$, 1-way ANOVA). (**K**) Protein levels and quantification of IBA1 and CD68 in control and EAU mice (mean ± SD; $n = 3$/group; $^{*}P < 0.05$, $^{**}P < 0.01$, unpaired Student's t-test). (**L**) Protein levels and quantification of IBA1 and CD68 between EAU mice and EAU mice with Muscone (mean ± SD; $n = 3$/group; $^{*}P < 0.05$, unpaired Student's t-test).

Investigative Ophthalmology & Visual Science

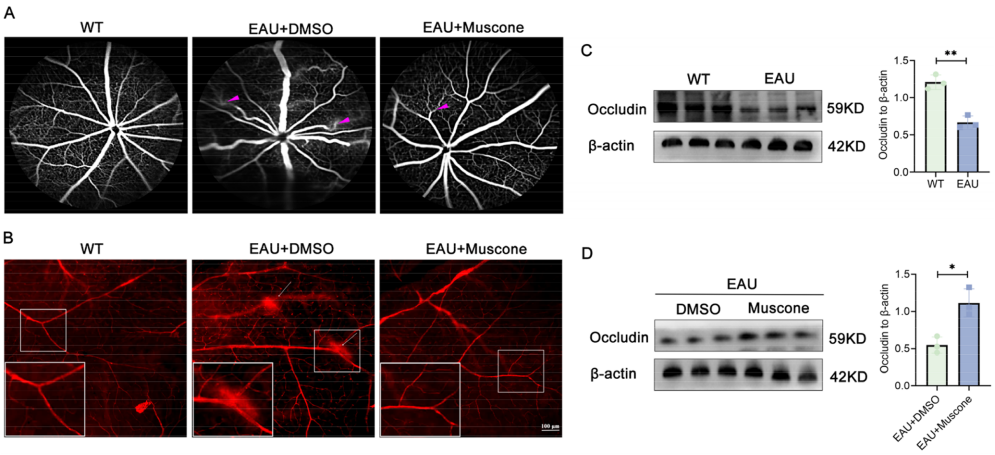

Figure 2. Muscone protects the integrity of the BRB. (**A**) Representative images of control mice, EAU mice, and EAU mice treated with Muscone following intraperitoneal injection of FFA (*purple triangle* = blood vessel curvature and leakage). (**B**) Evans blue staining images for the three groups mentioned above (*white arrow* = retinal vascular leakage). (**C**) Quantitative analysis of Occludin protein levels in the retinas of control and EAU mice (mean ± SD; $n = 3$/group; $^{**}P < 0.01$, unpaired Student's *t*-test). (**D**) Comparative quantitative analysis of Occludin protein levels in the retinas of EAU mice with and without Muscone treatment (mean ± SD; $n = 3$/group; $^{*}P < 0.05$, unpaired Student's *t*-test).

Muscone Inhibits the M1 Polarization of Microglia In Vitro

In vitro experiments using BV2 cells demonstrated the effect of Muscone on microglia. CCK8 assays at concentrations of 0.1, 1, 5, and 10 µM showed no cytotoxicity, with 0.1 µM and 1 µM selected for further experiments (Supplementary Fig. S2). The EdU555 assay indicated enhanced proliferation of BV2 cells after LPS and IFN-γ stimulation, which was reduced by Muscone treatment at 0.1 µM and 1 µM (Figs. 3A, 3B). Similarly, Muscone at these concentrations decreased the increased migratory capacity of BV2 cells under inflammatory conditions (Figs. 3C, 3D). Western blot analysis revealed elevated protein levels of inflammatory mediators (iNOS, IL-6, and IL-1β) in response to LPS and IFN-γ, which were decreased by Muscone treatment (Figs. 3E–3H). Consistently, the Nitric Oxide Test Kit showed increased nitric oxide levels in the LPS and IFN-γ group, reduced by Muscone treatment (Fig. 3I). These results suggest that Muscone may have anti-inflammatory effects by suppressing BV2 cell activation and proliferation under inflammatory conditions.

Muscone Alleviates Inflammation Through the p-PI3K/p-AKT Pathway In Vivo and In Vitro

To explore how Muscone reduces EAU inflammation, we performed Data-independent acquisition (DIA) proteomics on retinal tissues from EAU + DMSO mice and Muscone-treated EAU mice (Fig. 4A). Violin plots showed good experimental repeatability and strong sample correlation (Supplementary Fig. S3A). Kyoto Encyclopedia of Genes and Genomes (KEGG) analysis of total proteins revealed significant enrichment in metabolic pathways (Fig. 4B), suggesting a link between EAU and metabolism. Comparing the 2 groups, 74 proteins were upregulated and 203 downregulated in Muscone-treated mice ($P < 0.05$, fold change > 1.5; Fig. 4C). Many down-regulated proteins were related to inflammation, such as TLR2, TLR6, IRF7, C1qc, AHR, etc. A circular heatmap detailed all differentially expressed proteins (Fig. 4D).

Further, differential proteins of GO analysis indicated that Muscone impacts the downregulation of various aspects of the immune response, the immune system process as well as the innate immune response (Fig. 4E). Chord diagram of the relationship between differential proteins and pathways was showed (Fig. 4F). The top 10 of KEGG pathway analysis, in particular, highlighted the downregulation of the PI3K-AKT signaling pathway (Fig. 4G), a key player in mediating immune responses. We thus investigated this pathway further. Protein expression related to PI3K-AKT signaling was shown (Supplementary Figs. S3B–3M). Western blot revealed significantly decreased p-PI3K and p-AKT levels in the EAU + Muscone group as compared with the EAU + DMSO group (Fig. 4H). Similarly, in BV2 cells, Muscone reduced p-PI3K and p-AKT levels induced by LPS + IFN-γ (Fig. 4I).

PI3K Selective Inhibitor Attenuates EAU Inflammation

LY294002, a selective PI3K inhibitor,[30,31] is reported in numerous references to have an effective concentration of 10 µM.[32–34] Then, it was administered intravitreally at days 9 and 11 after immunized. At day 14, the development of EAU phenotype was observed. Clinical scores showed that inhibiting PI3K with LY294002 alleviated the ciliary congestion (Figs. 5A, 5B). Pathological evaluations revealed a decrease in inflammatory infiltrates following treatment with LY294002 (Figs. 5C, 5D). FFA suggested that the destruction of BRB was attenuated in LY294002 treated EAU mice (Fig. 5E). Additionally, the protein levels of iNOS and IL-6 were significantly decreased in the retinas of EAU mice treated with LY294002 (Fig. 5F).

Collectively, our results suggested that Muscone significantly alleviates inflammation associated with EAU via the PI3K-AKT pathway (Fig. 5G).

Investigative Ophthalmology & Visual Science

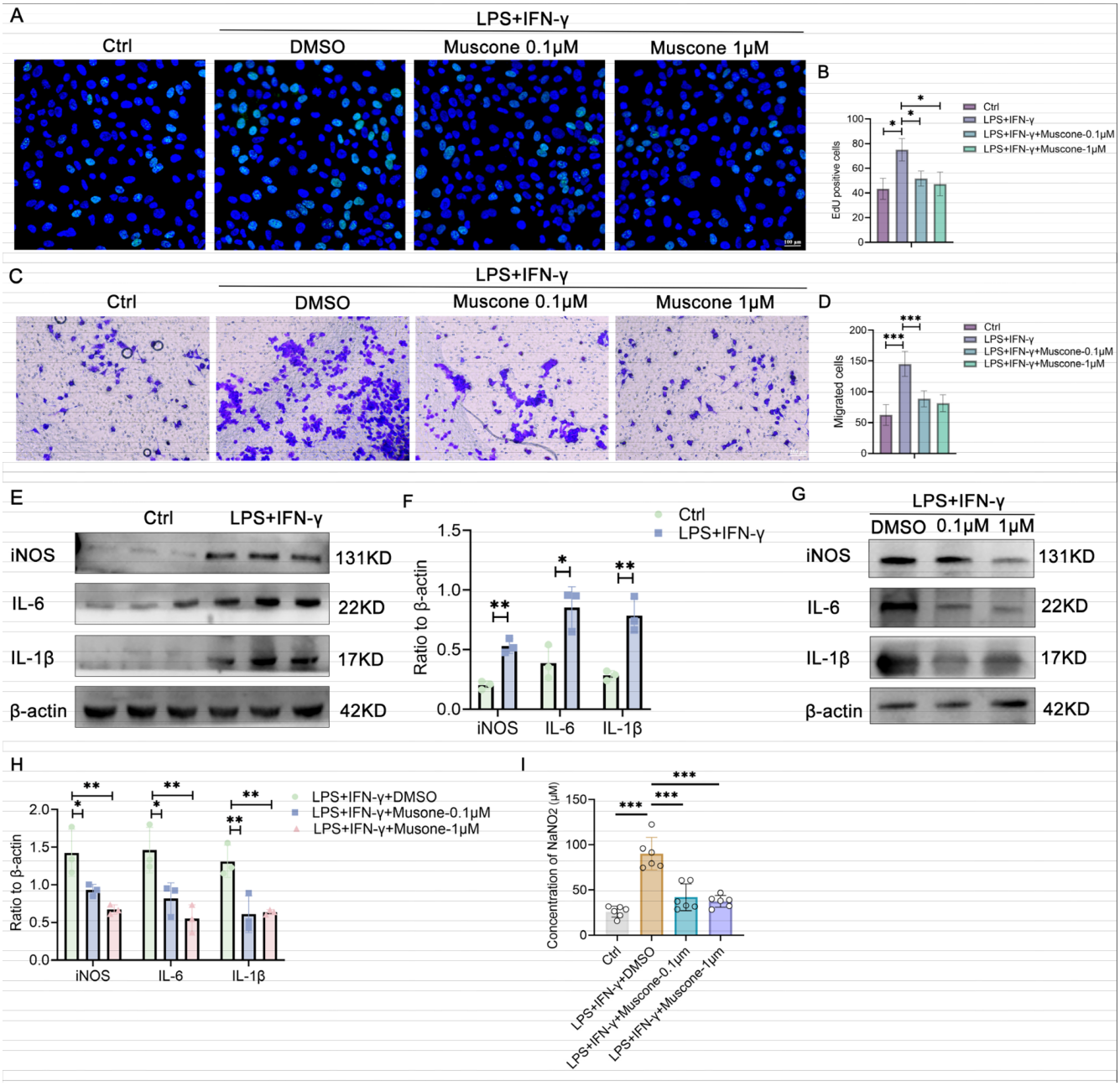

Figure 3. Muscone exerts an inhibitory effect in activated BV2 cells. (**A, B**) EdU555 assay for the control, LPS + IFN-γ treated, and LPS + IFN-γ treated with 0.1 μM or 1 μM Muscone (mean ± SD; $n = 3$/group; $^{*}P < 0.05$, $^{***}P < 0.001$, 1-way ANOVA). (**C, D**) Transwell assay and quantitative analysis for the four groups described (mean ± SD; $n = 4$/group; $^{***}P < 0.001$, 1-way ANOVA). (**E, F**) Protein levels and quantitative analysis of iNOS, IL-6, and IL-1β in BV2 cells with or without LPS + IFN-γ stimulation (mean ± SD; $n = 3$/group; $^{*}P < 0.05$, $^{**}P < 0.01$, unpaired Student's t-test). (**G, H**) Protein levels and quantification of iNOS, IL-6, and IL-1β protein levels in LPS + IFN-γ stimulated BV2 cells treated with DMSO, 0.1 μM or 1 μM Muscone (mean ± SD; $n = 3$/group; $^{**}P < 0.01$, unpaired Student's t-test). (**I**) Measurement of NaNO2 concentration in the control, LPS + IFN-γ, LPS + IFN-γ + 0.1 μM Musocne, LPS + IFN-γ + 1 μM Muscone groups (mean ± SD; $n = 5$/group; $^{***}P < 0.001$, 1-way ANOVA).

Discussion

Uveitis is a prevalent ocular condition that poses a significant risk of blindness, affecting individuals across all age groups but showing a marked predilection for young people.[35] The management of uveitis presents a formidable challenge, with no universally effective or targeted clinical therapies available, largely due to the intricate and multifactorial nature of its etiology and pathogenesis. While traditional glucocorticoids and a range of immunosuppressants can achieve a degree of symptom management, they are not without severe side effects.[36,37] Consequently, the quest for therapeutic agents that can prevent relapses, mitigate medication side effects, and maintain treatment efficacy has become a critical and pressing issue in clinical management.

Muscone, a derivative of the musk glands of musk animals, is a medicinal substance renowned for its potent pharmacological properties. Extensive research indicates

Investigative Ophthalmology & Visual Science

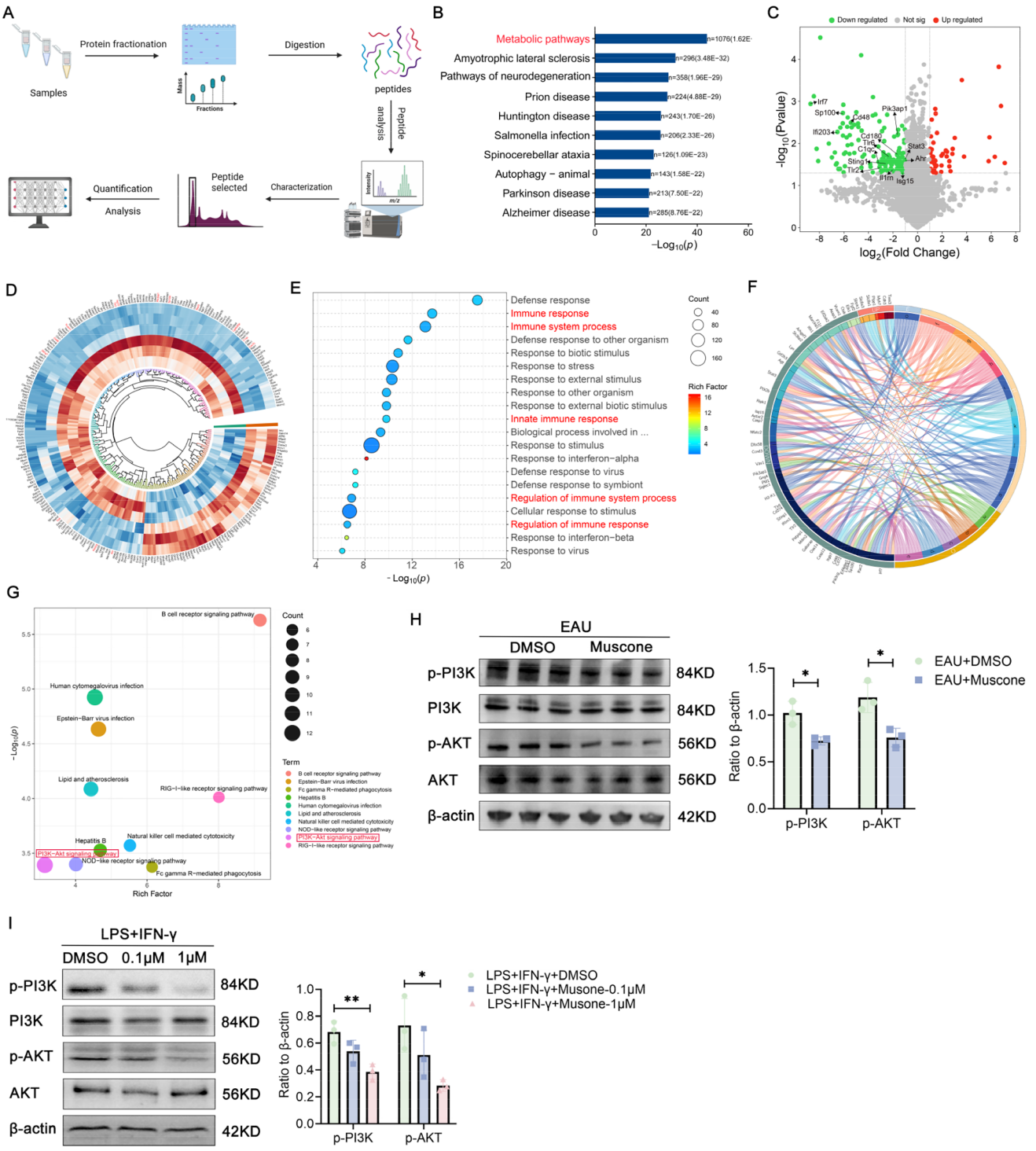

Figure 4. Muscone exhibits anti-inflammatory properties by modulating the PI3K/AKT signaling pathway. (**A**) Overview of the DIA experimental workflow. (**B**) KEGG pathway analysis of total proteins identified by LC-MS. (**C**) Volcano plot derived from DIA proteomics data. (**D**) Circular heatmap of significantly differential proteins. (**E**) Top 20 GO terms of the data. (**F**) Chord diagram illustrating the interconnectivity between differential proteins and their respective pathways. (**G**) Top 10 KEGG pathways. (**H**) Quantitative analysis of PI3K, p-PI3K, AKT, and p-AKT protein levels in the retinas of EAU mice with and without Muscone treatment (mean ± SD; $n = 3$/group; $^{*}P < 0.05$, unpaired Student's t-test). (**I**) Analysis of PI3K, p-PI3K, AKT, and p-AKT protein levels in LPS + IFN-γ treated BV2 cells with DMSO, 0.1 μM Muscone, and 1 μM Muscone (mean ± SD; $n = 3$/group; $^{*}P < 0.05$, $^{**}P < 0.01$, unpaired Student's t-test).

that Muscone possesses therapeutic benefits across a spectrum of diseases, impacting both the central nervous and cardiovascular systems.[17,18] Notably, Muscone exhibits robust anti-inflammatory action, capable of modulating the secretion of inflammatory cytokines like IL-1β and IL-6. Furthermore, Muscone plays a role by regulating membrane fluidity, MMP9 expression, and Na+, K (+)-ATPase activity in cells, thereby increasing the permeability of the blood-

Investigative Ophthalmology & Visual Science

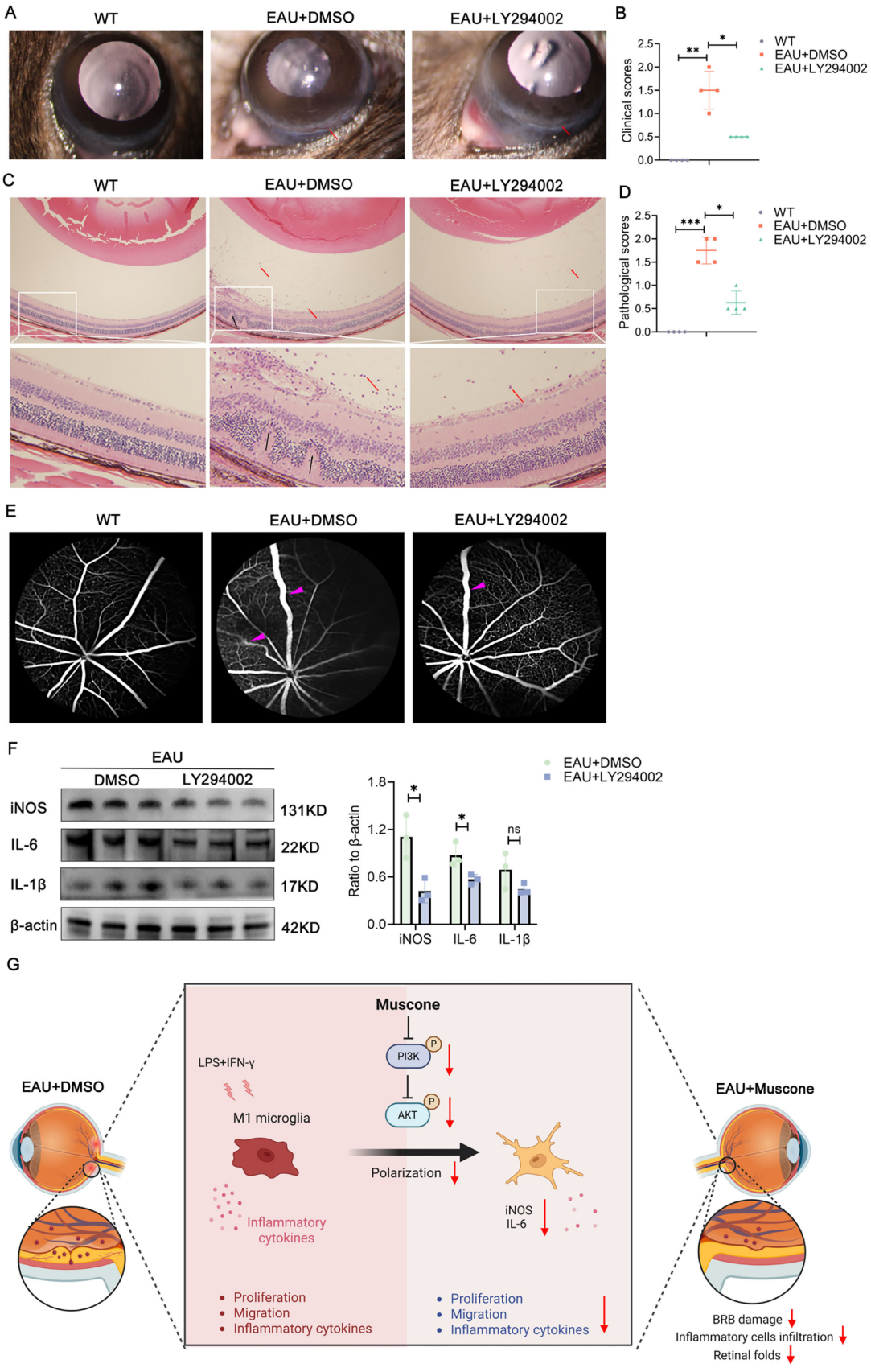

Figure 5. A PI3K-selective inhibitor effectively reduces inflammation in EAU. (**A, B**) Clinical scores of control mice, EAU mice with DMSO, EAU mice intravitreal injection with LY294002 (mean ± SD; $n = 4$/group; *$P < 0.05$, ***$P < 0.001$; Mann-Whitney U test; *red arrow* = ciliary congestion). (**C, D**) Pathological scores in the same groups mentioned above (mean ± SD; $n = 4$/group; *$P < 0.05$, **$P < 0.01$; Mann-Whitney U test; *red arrow* = inflammatory cells, *black arrow* = retinal folds). (**E**) Representative images from three groups intraperitoneal

FFA injection (*purple triangle* = blood vessel curvature and leakage). (**F**) The protein level and quantification of iNOS, IL-6, and IL-1β in the retinas of EAU mice with LY294002 (mean ± SD; n = 3/group; ns > 0.05, *P < 0.05, unpaired Student's t-test). (**G**) The function and mechanism of Muscone in EAU.

brain or BRB, exerting a direct anti-inflammatory effect at the site of pathology.[38,39]

Considering that multiple studies reporting that the regulation of microglia activation can reduce the severity of EAU,[40–42] targeting microglia for the treatment of uveitis has been a research hotspot.[41,43,44] In this study, we identified that Muscone could play a powerful therapeutic effect on EAU through the PI3K/AKT pathway in BV2 cells.

Building on prior research indicating that inflammation peaks on day 14 after immunization,[45] we selected this time point to evaluate Muscone's efficacy. We administered Muscone intraperitoneally at 20 mg/kg from day 7 to day 14, every other day. Our findings revealed that Muscone alleviated BRB disruption and reduced inflammatory cytokine levels in retinas. In vitro experiments also demonstrated that Muscone blocked BV2 cell activation and downregulated inflammatory factors.

To further investigate the specific mechanism of Muscone attenuating EAU mice, we performed proteomic and LC-MS analysis with the retinas from EAU + DMSO and EAU + Muscone mice on day 14 after induction. GO analysis indicated that Muscone affected the downregulation of innate immune responses. In consistently with GO analysis, Muscone could inhibit the activation of microglial cells, which are the major innate immune cells in the eye.[29] KEGG analysis revealed a significant downregulation of the PI3K/AKT signaling pathway, which is a classic immune-related pathway that plays important roles in various autoimmune diseases.[46–48] PI3Ks are a family of heterodimeric lipid kinases. AKT is one kind of serine protein kinase from the protein kinase AGC subfamily and acts as one of essential downstream factors of PI3K.[49] PI3K/AKT is widely regarded as an important pathway to trigger several biochemical reactions that are closely related to metabolism and disease occurrence. Some autoimmune diseases, such as rheumatoid arthritis and multiple sclerosis, show increased activity of the PI3K/AKT pathway.[50,51] Here, subsequent Western blotting confirmed that the expression of p-PI3K/p-AKT was upregulated in EAU, and Muscone could downregulate the expression of p-PI3K/p-AKT both in vivo and in vitro. Furthermore, after intravitreal injection of PI3K selective inhibitor LY294002, we observed reduced inflammatory phenotypes in EAU.

In this study, there are still some limitations. In the retina of EAU mice, other cell types besides microglia, such as macrophages and RPE cells, also express inflammatory chemokines and cytokines. Western blotting, while useful for assessing overall protein expression, cannot distinguish the specific cell types responsible for expressing these proteins. Acknowledging these limitations, flow cytometry or confocal microscopy are needed to further validate muscone's effects on microglia in the future study. The data mentioned are derived from in vivo animal models and in vitro cell models. However, our current understanding is limited by the absence of clinical data, as we have not yet evaluated the effects of Muscone in clinical trials involving human patients. Further study is planned to bridge this gap with clinical studies. Additionally, whereas our proteomic analysis has revealed numerous downstream proteins potentially regulated by Muscone, the inherent structural limitations of Muscone preclude a straightforward verification of direct interactions with these targets. Consequently, the specific molecular targets that are directly engaged by Muscone remain to be elucidated. Furthermore, the current experimental design for constructing EAU mouse models is limited by the exclusive use of female subjects. To better mirror the heterogeneous nature of uveitis presentation in human populations and enhance the clinical relevance of our findings, future in vivo studies will incorporate both male and female mice in experimental cohorts.

In conclusion, we demonstrated that Muscone could alleviate autoimmune uveitis via the PI3K/AKT pathway.

Acknowledgments

The authors thank members of the Beijing Institution of Ophthalmology for their invaluable support and guidance throughout this research project.

Supported by the National Natural Science Foundation Project of China (82271078 and 82371045), Youth Beijing Scholar (No. 076), Beijing Municipal Public Welfare Development and Reform Pilot Project for Medical Research Institutes (PWD & RPP-MRI and JYY2023-6), the Chongqing Natural Science Foundation (CSTB2022NSCQ-MSX0144).

Author Contributions: X.L., H.Z., and C.W. designed the research, performed the study. Q.Z. and F.L. provided analysis tools and experiments protocols. N.L., F.C., and K.H. helped to polish manuscript. B.C., S.Z., H.F., and Y.W. contributed reagents and materials. S.H. conceived the research and revised the manuscript. Authors have read and approved the final manuscript.

Data Availability Statements: The authors declare that all the data supporting the findings of this study are available in the manuscript.

Disclosure: **X. Liu**, None; **H. Zuo**, None; **C. Wu**, None; **N. Li**, None; **Q. Zhou**, None; **F. Cao**, None; **B. Chu**, None; **S. Zeng**, None; **H. Feng**, None; **Y. Wang**, None; **F. Lei**, None; **K. Hu**, None; **S. Hou**, None

References

1. Joltikov KA, Lobo-Chan AM. Epidemiology and risk factors in non-infectious uveitis: a systematic review. *Front Med (Lausanne)*. 2021;8:695904.
2. Burek-Michalska A, Turno-Kręcicka A. Adalimumab in the treatment of non-infectious uveitis. *Adv Clin Exp Med*. 2020;29(10):1231–1236.
3. Bertrand PJ, Jamilloux Y, Ecochard R, et al. Uveitis: autoimmunity… and beyond. *Autoimmun Rev*. 2019;18(9):102351.
4. Triggianese P, Fatica M, Caso F, et al. Rheumatologist's perspective on non-infectious uveitis: patterns from tertiary referral rheumatologic clinics in Italy. *Int J Mol Sci*. 2023;24(11):9690.
5. Liu X, Meng J, Liao X, et al. A de novo missense mutation in MPP2 confers an increased risk of Vogt-Koyanagi-Harada disease as shown by trio-based whole-exome sequencing. *Cell Mol Immunol*. 2023;20(11):1379–1392.

6. Egwuagu CE, Alhakeem SA, Mbanefo EC. Uveitis: molecular pathogenesis and emerging therapies. *Front Immunol*. 2021;12:623725.
7. Balasubramaniam B, Chong YJ, Azzopardi M, Logeswaran A, Denniston AK. Topical anti-inflammatory agents for non-infectious uveitis: current treatment and perspectives. *J Inflamm Res*. 2022;15:6439–6451.
8. Valdes LM, Sobrin L. Uveitis therapy: the corticosteroid options. *Drugs*. 2020;80(8):765–773.
9. Letko E, Yeh S, Foster CS, Pleyer U, Brigell M, Grosskreutz CL. Efficacy and safety of intravenous secukinumab in noninfectious uveitis requiring steroid-sparing immunosuppressive therapy. *Ophthalmology*. 2015;122(5):939–948.
10. Emmi G, Bettiol A, Hatemi G, Prisco D. Behçet's syndrome. *Lancet*. 2024;403(10431):1093–1108.
11. Schwartzman S, Schwartzman M. The use of biologic therapies in uveitis. *Clin Rev Allergy Immunol*. 2015;49(3):307–316.
12. Wang J, Wong YK, Liao F. What has traditional Chinese medicine delivered for modern medicine? *Expert Rev Mol Med*. 2018;20:e4.
13. Wang Y, Shi X, Li L, Efferth T, Shang D. The impact of artificial intelligence on traditional Chinese medicine. *Am J Chin Med*. 2021;49(6):1297–1314.
14. Zhao L, Zhang H, Li N, et al. Network pharmacology, a promising approach to reveal the pharmacology mechanism of Chinese medicine formula. *J Ethnopharmacol*. 2023;309:116306.
15. Wang WJ, Zhang T. Integration of traditional Chinese medicine and Western medicine in the era of precision medicine. *J Integr Med*. 2017;15(1):1–7.
16. Wang J, Xing H, Qin X, Ren Q, Yang J, Li L. Pharmacological effects and mechanisms of muscone. *J Ethnopharmacol*. 2020;262:113120.
17. Wu Q, Li H, Wu Y, et al. Protective effects of muscone on ischemia-reperfusion injury in cardiac myocytes. *J Ethnopharmacol*. 2011;138(1):34–39.
18. Han B, Zhao Y, Yao J, et al. Proteomics on the role of muscone in the "consciousness-restoring resuscitation" effect of musk on ischemic stroke. *J Ethnopharmacol*. 2022;296:115475.
19. Li L, Wang N, Jin Q, Wu Q, Liu Y, Wang Y. Protection of Tong-Qiao-Huo-Xue decoction against cerebral ischemic injury through reduction blood-brain barrier permeability. *Chem Pharm Bull (Tokyo)*. 2017;65(11):1004–1010.
20. Li D, Chen B, Zhang L, et al. The musk chemical composition and microbiota of Chinese forest musk deer males. *Sci Rep*. 2016;6:18975.
21. Mattapallil MJ, Silver PB, Cortes LM, et al. Characterization of a new epitope of IRBP that induces moderate to severe uveoretinitis in mice with H-2b haplotype. *Invest Ophthalmol Vis Sci*. 2015;56(9):5439–5449.
22. Cortes LM, Mattapallil MJ, Silver PB, et al. Repertoire analysis and new pathogenic epitopes of IRBP in C57BL/6 (H-2b) and B10.RIII (H-2r) mice. *Invest Ophthalmol Vis Sci*. 2008;49(5):1946–1956.
23. Meng J, Liu X, Tang S, et al. METTL3 inhibits inflammation of retinal pigment epithelium cells by regulating NR2F1 in an m(6)A-dependent manner. *Front Immunol*. 2022;13:905211.
24. Tian L, Yang P, Lei B, et al. AAV2-mediated subretinal gene transfer of hIFN-α attenuates experimental autoimmune uveoretinitis in mice. *PLoS One*. 2011;6(5):e19542.
25. Agarwal RK, Silver PB, Caspi RR. Rodent models of experimental autoimmune uveitis. *Methods Mol Biol*. 2012;900:443–469.
26. Chen M, Luo C, Zhao J, Devarajan G, Xu H. Immune regulation in the aging retina. *Prog Retin Eye Res*. 2019;69:159–172.
27. O'Leary F, Campbell M. The blood-retina barrier in health and disease. *FEBS J*. 2023;290(4):878–891.
28. Rudraraju M, Narayanan SP, Somanath PR. Distinct mechanisms of human retinal endothelial barrier modulation in vitro by mediators of diabetes and uveitis. *Life (Basel)*. 2021;12(1):33.
29. Fan W, Huang W, Chen J, Li N, Mao L, Hou S. Retinal microglia: functions and diseases. *Immunology*. 2022;166(3):268–286.
30. Li J, Liu XG, Ge RL, et al. The ligation between ERMAP, galectin-9 and dectin-2 promotes Kupffer cell phagocytosis and antitumor immunity. *Nat Immunol*. 2023;24(11):1813–1824.
31. Ma M, Hua S, Min X, et al. p53 positively regulates the proliferation of hepatic progenitor cells promoted by laminin-521. *Signal Transduct Target Ther*. 2022;7(1):290.
32. Wang K, Kou Y, Rong X, et al. ED-71 improves bone mass in ovariectomized rats by inhibiting osteoclastogenesis through EphrinB2-EphB4-RANKL/OPG axis. *Drug Des Devel Ther*. 2024;18:1515–1528.
33. Wei J, Wang DF, Cui CC, Tan JJ, Peng MY, Lu HX. CXCL4/CXCR3 axis regulates cardiac fibrosis by activating TGF-β1/Smad2/3 signaling in mouse viral myocarditis. *Immun Inflamm Dis*. 2024;12(4):e1237.
34. Shi N, Wang Y, Xia Z, et al. The regulatory role of the apelin/APJ axis in scarring: identification of upstream and downstream mechanisms. *Biochim Biophys Acta Mol Basis Dis*. 2024;1870(4):167125.
35. Samalia PD, Lim LL, Niederer RL. Insights into the diagnosis and management of sarcoid uveitis: a review. *Clin Exp Ophthalmol*. 2024;52(3):294–316.
36. Wu X, Tao M, Zhu L, Zhang T, Zhang M. Pathogenesis and current therapies for non-infectious uveitis. *Clin Exp Med*. 2023;23(4):1089–1106.
37. Boonhaijaroen T, Choopong P, Tungsattayathitthan U, Tesavibul N, Sanphan W, Boonsopon S. Treatment outcomes in cytomegalovirus anterior uveitis. *Sci Rep*. 2024;14(1):15210.
38. Wang GY, Wang N, Liao HN. Effects of Muscone on the expression of P-gp, MMP-9 on blood-brain barrier model in vitro. *Cell Mol Neurobiol*. 2015;35(8):1105–1115.
39. Chen ZZ, Lu Y, Du SY, Shang KX, Cai CB. Influence of borneol and muscone on geniposide transport through MDCK and MDCK-MDR1 cells as blood-brain barrier in vitro model. *Int J Pharm*. 2013;456(1):73–79.
40. Wang G, Li X, Li N, et al. Icariin alleviates uveitis by targeting peroxiredoxin 3 to modulate retinal microglia M1/M2 phenotypic polarization. *Redox Biol*. 2022;52:102297.
41. Shu N, Zhang Z, Wang X, et al. Apigenin alleviates autoimmune uveitis by inhibiting microglia M1 pro-inflammatory polarization. *Invest Ophthalmol Vis Sci*. 2023;64(5):21.
42. Li W, He S, Tan J, et al. Transcription factor EGR2 alleviates autoimmune uveitis via activation of GDF15 to modulate the retinal microglial phenotype. *Proc Natl Acad Sci USA*. 2024;121(39):e2316161121.
43. Huang J, Wang X, Li N, et al. YY1 lactylation aggravates autoimmune uveitis by enhancing microglial functions via inflammatory genes. *Adv Sci (Weinh)*. 2024;11(19):e2308031.
44. Wang Y, Gao S, Cao F, Yang H, Lei F, Hou S. Ocular immune-related diseases: molecular mechanisms and therapy. *MedComm (2020)*. 2024;5(12):e70021.
45. Okunuki Y, Mukai R, Nakao T, et al. Retinal microglia initiate neuroinflammation in ocular autoimmunity. *Proc Natl Acad Sci USA*. 2019;116(20):9989–9998.
46. Zhou W, Qu H, Fu XX, et al. Neuroprotective effects of a novel peptide through the Rho-integrin-Tie2 and PI3K/Akt

Investigative Ophthalmology & Visual Science

pathways in experimental autoimmune encephalomyelitis model. *Front Pharmacol*. 2024;15:1290128.

47. Qi X, Lu X, Han Y, Xing Y, Zheng Y, Cui C. Ginseng polysaccharide reduces autoimmune hepatitis inflammatory response by inhibiting PI3K/AKT and TLRs/NF-κB signaling pathways. *Phytomedicine*. 2023;116:154859.
48. He C, Li Y, Gan L, et al. Notch signaling regulates Th17 cells differentiation through PI3K/AKT/mTORC1 pathway and involves in the thyroid injury of autoimmune thyroiditis. *J Endocrinol Invest*. 2024;47(8):1971–1986.
49. Yudushkin I. Getting the Akt together: guiding intracellular Akt activity by PI3K. *Biomolecules*. 2019;9(2):67.
50. Zheng Q, Liu L, Liu H, et al. The Bu Shen Yi Sui formula promotes axonal regeneration via regulating the neurotrophic factor BDNF/TrkB and the downstream PI3K/Akt signaling pathway. *Front Pharmacol*. 2019;10:796.
51. Chen Y, Li Z, Li H, et al. Apremilast regulates the Teff/Treg balance to ameliorate uveitis via PI3K/AKT/FoxO1 signaling pathway. *Front Immunol*. 2020;11:581673.